Biochemical Journal (2021) **478** 389–406
https://doi.org/10.1042/BCJ20200411

Research Article

Licochalcone A is a natural selective inhibitor of arginine methyltransferase 6

Shuai Gong[1], Shinji Maegawa[2], Yanwen Yang[2], Vidya Gopalakrishnan[2,3], Guangrong Zheng[4] and Donghang Cheng[2]

[1]Department of Oncology, the First Affiliated Hospital of Zhengzhou University, Zhengzhou University, Zhengzhou 450052, China; [2]Departments of Pediatrics, University of Texas, MD Anderson Cancer Center, Houston, TX 77030, U.S.A.; [3]Molecular and Cellular Oncology, University of Texas, MD Anderson Cancer Center, Houston, TX 77030, U.S.A.; [4]Department of Medicinal Chemistry, College of Pharmacy, University of Florida, Gainesville, FL, U.S.A

Correspondence: Vidya Gopalakrishnan (vgopalak@mdanderson.org) or Guangrong Zheng (zhengg@cop.ufl.edu) or Donghang Cheng (dcheng@mdanderson.org)

Arginine methylation is a post-translational modification that is implicated in multiple biological functions including transcriptional regulation. The expression of protein arginine methyltransferases (PRMT) has been shown to be up-regulated in various cancers. PRMTs have emerged as attractive targets for the development of new cancer therapies. Here, we describe the identification of a natural compound, licochalcone A, as a novel, reversible and selective inhibitor of PRMT6. Since expression of PRMT6 is up-regulated in human breast cancers and is associated with oncogenesis, we used the human breast cancer cell line system to study the effect of licochalcone A treatment on PRMT6 activity, cell viability, cell cycle, and apoptosis. We demonstrated that licochalcone A is a non-S-adenosyl L-methionine (SAM) binding site competitive inhibitor of PRMT6. In MCF-7 cells, it inhibited PRMT6-dependent methylation of histone H3 at arginine 2 (H3R2), which resulted in a significant repression of estrogen receptor activity. Licochalcone A exhibited cytotoxicity towards human MCF-7 breast cancer cells, but not MCF-10A human breast epithelial cells, by up-regulating p53 expression and blocking cell cycle progression at G2/M, followed by apoptosis. Thus, licochalcone A has potential for further development as a therapeutic agent against breast cancer.

Introduction

As one of the common protein post-translational modifications, arginine methylation plays an important role in a number of physiological processes and pathological conditions, including chromatin remodeling, transcriptional regulation, RNA processing, trafficking, signal transduction, DNA repair and RNA splicing in various cancers [1,2]. Arginine methylation can be mediated by a family of enzymes known as protein arginine methyltransferases (PRMTs), of which nine different members have been identified. PRMTs transfer a methyl-group from methyl-donor S-Adenosyl methionine (SAM) onto the terminal guanidino nitrogen atoms of arginines and are categorized into three sub-classes based on how the arginine residues are methylated. All PRMTs catalyze a ω-N^G-monomethylarginine (MMA), which is then utilized by Type I PRMTs (PRMT1, 2, 3, 4, 6 and 8) to further catalyze the production of ω-N^G,N^G-asymmetric dimethylarginine (ADMA) or by Type II PRMTs (PRMT5, 9) to catalyze the formation of ω-N^G,N'^G-symmetric dimethylarginine (SDMA) [1]. PRMT7 is a Type III enzyme and is the only member in the sub-class to catalyze MMA formation [2].

PRMT6 is a predominantly nuclear enzyme characterized by its distinct substrates specificity and by its automethylation, which plays an important role for its stability and activity [3–5]. Kinetic studies have attributed a distributive rather than processive mode of action to PRMT6 in its catalysis of demethylation of targets [6]. Histones comprise a major set of substrates of PRMT6 [3]. It is the

Received: 29 May 2020
Revised: 17 November 2020
Accepted: 27 November 2020

Accepted Manuscript online: 27 November 2020
Version of Record published: 27 January 2021

Biochemical Journal (2021) **478** 389–406
https://doi.org/10.1042/BCJ20200411

primary enzyme to mediate asymmetric methylation of H3R2 in mammalian cells [7–9]. This modification interferes with transcriptional activation associated with trimethylation of histone H3 at lysine (K)-4 (H3K4me3) [7]. It is involved in partial blockade of the recruitment of WD repeat family (WDR5) protein, a subunit of the mixed lineage leukemia (MLL) complex, to promoters [7–9]. PRMT6 elevation and increased H3R2me2a methylation, has also been shown to interfere with the effector functions of the Inhibitor of Growth (ING), a reader of H3K4me3, and a tumor suppressor down-regulated in a variety of cancers [9,10]. p53 is an important target of the repressive activity of PRMT6 [11]. PRMT6 controls p53 expression by directly binding its promoter to silence its expression, and indirectly by repressing the expression of HOXA10, a positive regulator of p53 [8,11,12]. Consistent with this, knockout or knockdown of PRMT6 up-regulates p53 expression, thus, likely that in tumors with high PRMT6 levels, the p53 pathway is epigenetically silenced [11,13]. Thrombospondin-1 (TSP-1), a potent natural inhibitor of angiogenesis, is also transcriptionally repressed by PRMT6, and reduction in TSP-1 level promotes tumor progression [14,15].

Besides its activity at H3R2, PRMT6 can also methylate histones H4 and H2A at R3 and histone H3 at R17 sites [8,16]. This has been proposed as a mechanism by which PRMT6 functions as a transcriptional coactivator of the nuclear receptors [17]. Beyond histone substrates histone substrates, non-histone substrates of PRMT6 have also been described, including the nuclear scaffold protein HMGA1a/b [18,19], DNA polymerase beta [20], tumor suppressor p16, p21, and PTEN [21–23]. Thus, arginine methylation by PRMT6 plays multiple roles in cellular activities including chromatin remodeling, transcriptional regulation, RNA processing, signal transduction, DNA repair and RNA splicing [9,17,19,24].

PRMT6 expression is up-regulated in various human malignancies, including bladder, lung, and breast cancer [26,27], and its elevation is correlated with poor prognosis for patients with breast, colon, or lung cancers [4,13,28]. Recent data using genetically engineered mice provide compelling support for an oncogenic role for PRMT6 in mammary gland tumorigenesis, suggesting that it may be a good therapeutic target [29]. However, only a few studies have reported on the pre-clinical development of PRMT6 inhibitors [30–32].

Licochalcone A, one of the main flavonoids extracted from licorice root has shown broad anti-inflammatory, antibacterial, anticancer, and antioxidative bioactivities [33]. Although, the cytotoxic effect of licochalcone A against a number of cancers including breast has been tied to induction of apoptosis, cell cycle arrest, and autophagy [34–37], its exact cytotoxic mechanism remains elusive. We had previously identified licochalcone A as a PRMT inhibitor [38]. Here, we performed the first detailed biochemical characterization of licochalcone A-PRMT6 interaction and connected the reduction in viability of breast cancer cells to the up-regulation of p53 expression and the induction of cell cycle arrest and apoptosis in response to drug treatment. To our knowledge, we are the first to identify a natural inhibitor with higher specificity towards PRMT6.

Materials and methods

Plasmids, antibodies, and chemicals

All GST fusion proteins were subcloned into *pGEX6P-1*, which allows for the induced production of recombinant proteins fused to the C terminus of glutathione S-transferase including: GST-PRMT1, GST-PRMT3, GST-CARM1, and GST-PRMT6, as previously described [3]. GST-Npl3 was a gift from Pam Silver (Harvard Medical School, MA, U.S.A.) [39]. GST-Suv39H1 was a gift from Thomas Jenuwein (Max-Planck Institute of Immunobiology, Freiburg, Germany) [40]. GST-SET7 was a gift from Yi Zhang (Lineberger Comprehensive Cancer Center, Chapel Hill, U.S.A.) [41]. GST-G9a was a gift from Yoichi Shinkai (Institute for Virus Research, Kyoto, Japan) [42]. Myc-PRMT5 and pVAX-PRMT6 were gifts from Stephane Richard (Lady Davis Institute for Medical Research, Montreal, Canada). FLAG tagged human PRMT6 cDNA was cloned into a pCAGGS vector. Histones H3 and H4 from calf thymus were purchased from Roche Applied Science. The following antibodies were employed: anti-FLAG and anti-β-actin antibodies (Sigma–Aldrich, St. Louis, MO, U.S.A.), anti-c-Myc antibody (Covance, Denver, PA, U.S.A.), anti-CARM1 and anti-PRMT6 antibodies (Bethyl Laboratories, Montgomery, TX, U.S.A.), anti-p53 antibody (Santa Cruz Biotechnology, Santa Cruz, CA, U.S.A.), anti-cleaved caspase-3 and anti-cleaved PARP antibodies (Cell Signaling Technology, Beverly, MA), anti-H4R3me2a and anti-H3K9me3 antibodies (Active Motif, Rixensart, Belgium), anti-H3R2m1 and anti-H3R2m2a antibodies (Abcam, Cambridge, U.K.) and anti-H3R17me2a antibody (MED Millipore, Burlington, MA, U.S.A.). Licochalcone A and Sinefungin were purchased from ALEXIS Corporation (San Diego, CA, U.S.A.) and Sigma–Aldrich (St. Louis, MO, U.S.A.), respectively.

Biochemical Journal (2021) 478 389–406
https://doi.org/10.1042/BCJ20200411

In vitro methylation assay and IC_{50} determination

Assays have been described in detail previously [40]. All methylation assays were carried out in a final volume of 30 μl of PBS and in the presence of S-adenosyl-L-[methyl-^{3}H] methionine ([^{3}H]AdoMet, 85 Ci/mmol from a 0.5 mCi/ml in dilute HCl/ethanol 9:1, pH 2.0–2.5, PerkinElmer Life Sciences, Waltham, MA, U.S.A.). Specific information pertaining to individual reaction conditions is described in each of the figure legends. The reactions contained substrate (0.5–1.0 μg) and recombinant enzyme (0.1–0.5 μg) with 50 μM of each compound or different doses of licochalcone A for IC_{50} determination. The mixtures were incubated at 30°C for 90 min and then resolved by SDS–PAGE, transferred to a PVDF membrane, sprayed with Enhance (PerkinElmer Life Sciences. Waltham, MA, U.S.A.), and exposed to film overnight for fluorography. Briefly, after *in vitro* methylation reactions, the samples were resolved by SDS–PAGE transferred to a PVDF membrane, stained with Ponceau S, and the visualized bands of substrate were cut out, the disintegration per minute (dpm) was determined by using a liquid scintillation analyzer (Tri-Carb, Packard, Ramsey, MN, U.S.A.), and the IC_{50} values were calculated.

Cell lines and cultures

The tamoxifen-inducible *PRMT1*$^{fl/-}$ER-Cre MEFs and the MCF-7-Tet-on-*shCARM1* cell lines have been described previously [43]. MCF-7 and MCF-10A cell lines were obtained from ATCC. MCF-10A cells were cultured in DMEM/F12 Ham's Mixture supplemented with 5% horse serum (Thermo Fisher Scientific, Waltham, MA, U.S.A.), EGF 20 ng/ml (Sigma–Aldrich, St. Louis, MO, U.S.A.), insulin 10 μg/ml (Sigma–Aldrich), hydrocortisone 0.5 mg/ml (Sigma–Aldrich), cholera toxin 100 ng/ml (Sigma–Aldrich). The other cell lines were maintained in Dulbecco's Modified Eagle's Medium (DMEM) containing fetal bovine serum (10%).

Photoaffinity competition labeling of methyltransferase enzymes

UV cross-linking of S-adenosyl-L-[methyl-3H] methionine to PRMT6 was performed as previously described [44]. A CL-1000 UV cross-linker was used (UVP, Upland, CA, U.S.A.). GST-PRMT6 (10 μg) without any competitor or with 200 μM sinefungin, 200 μM licochalcone A, 200 μM AMI-5, respectively, was exposed to UV light (254 nm) at a distance of 1 cm for 30 min at 4°C in the presence of 3.2 μM [^{3}H]AdoMet and 5 mM dithiothreitol in a total volume of 50 μl of PBS. After UV cross-linking, samples were run on SDS–PAGE and subjected to fluorography. Ponceau S staining of the same membrane served a loading control.

Cellular thermal shift assay

The assay was performed as detailed previously [45]. The assay measures the ability of compound to interact with, and stabilize targets in intact cells. Briefly, MCF-7 cells cultured in 10 cm dishes at 90% confluency were treated with dimethyl sulfoxide (DMSO) or licochalcone A for 24 h. After treatment, cells were detached with trypsin, collected by centrifugation and subsequently resuspended in PBS. They were then aliquoted, and the aliquots were heated to different temperatures (40–64°C) for 3 min, cooled at room temperature for 2 min and placed on ice. Cells were lysed by three freeze/thaw cycles in liquid nitrogen. Insoluble proteins were separated by centrifugation, and the soluble fractions were used for SDS–PAGE and Western blotting.

Cell viability assay

CellTiter-Glo luminescent reagent (Promega, Madison, WI, U.S.A.) were used to determine cell viability according to the manufacturer's protocol.

Luciferase assay

Dox-inducible *CARM1* knockdown MCF-7 cells were cultured in phenol red-free DMEM supplemented with 10% charcoal stripped fetal calf serum. Cells were seeded in 24-well culture dishes. Dox-inducible *CARM1* knockdown MCF-7 cells were treated with 1 μg/ml of doxycycline for 6 days (d) to knockdown endogenous *CARM1* expression. Cells in each well were transfected with Lipofectamine 2000 transfection reagent (Thermo Fisher Scientific, Waltham, MA, U.S.A.) according to the manufacturer's protocol. MCF-7 and Dox-inducible *CARM1* knockdown MCF-7 cells were transiently transfected with 250 ng of *ERE-LUC*, 200 ng of *pSG-GRIP1*, 200 ng of *pVAX-PRMT6*, and 2 ng humanized CMV-Renilla internal control. After 12 h of transfection, cells were treated with 20 nM E2 to induce ERE-firefly and indicated amount of licochalcone A for 36 h. The cells were washed twice with PBS and harvested. Passive lysis of cells that lysed in Passive Lysis

Biochemical Journal (2021) 478 389–406
https://doi.org/10.1042/BCJ20200411

Buffer were used to perform luciferase assay using the Dual Luciferase Assay System (Promega, Madison, WI, U.S.A.) and western blotting. Relative activity of firefly luciferase was normalized against Renilla luciferase activity.

Quantitative reverse transcription PCR (RT-qPCR)

MCF-7 cells were cultured in phenol red-free DMEM supplemented with 10% charcoal dextran-stripped FBS for 4 days before treatment. After 24 h of indicated amount of licochalcone A treatment, medium was changed and cells were treated with 20 nM E2 to induce ER transcriptional activation and the same amount of licochalcone A. After 24 h, total RNA was extracted using RNeasy Mini kit (Qiagen, Mississauga, ON, Canada) and cDNA was synthesized using iScript cDNA Synthesis Kits system (Bio-Rad Laboratories, Hercules, CA, U.S.A.). qPCR was then performed using primer sets against the specified genes (Supplementary Table S1). Data was analyzed using the Sequence Detection System software (Bio-Rad). The experimental cycle threshold (Ct) was calibrated against the β-actin control product, and the amount of sample product from licochalcone A-treated cells relative to that of the control cells was determined using the DDC_t method (1-fold, 100%).

Cell cycle analysis

The effect of licochalcone A on cell cycle distribution was examined using propidium iodide (PI) as a DNA stain to determine DNA content by flow cytometry. MCF-7 and MCF-10A cells were treated with licochalcone A at the indicated concentrations for 48 h. Following the licochalcone A treatment, cells were harvested and washed three times with PBS, and fixed in 70% ethanol at −20°C overnight. Then, the cells were resuspended in 1 ml of PBS containing 20 μg/ml RNase A and 20 μg/ml PI. Cells were incubated in the dark for 3 h at 4°C. The cells were subjected to cell cycle analysis using a flow cytometer (BD LSRFortessa Flow Cytometer, San Jose, CA, U.S.A.).

Cell apoptosis analysis

Apoptotic cell death was quantified by a flow cytometer using the FITC Annexin V Apoptosis Detection Kit with 7-AAD (BioLegend, San Jose, CA, U.S.A.), according to the manufacturer's instruction. In brief, MCF-7 and MCF-10A cells were treated with licochalcone A (10, 30 or 40 μM) or vehicle (DMSO) for 48 h. Cells were then harvested, washed twice with ice-cold PBS. The washed cell samples were incubated with Annexin-V and 7-AAD for 15 min in the dark, then evaluated for apoptosis using a BD LSRFortessa Flow Cytometer. A total of 10 000 cells were collected and analyzed. Cells that stain positive for annexin V and negative for 7-AAD are undergoing early apoptosis; cells that stain positive for both annexin V and 7-AAD are either in the late stage of apoptosis, undergoing necrosis, or already dead.

Gene expression profile in patient samples

Microarray datasets containing the gene expression values of patients with breast cancer were obtained from Gene Expression Omnibus (www.ncbi.nlm.nih.gov/geo). The GSE29431 dataset, which contained Affymetrix Human Gene U133 Plus 2.0 Array profiling of 12 normal breast tissues and 54 primary breast carcinoma samples, were used to evaluate gene expression [46]. Microarray data were normalized using the robust multiarray average method. The expression data for each gene were Z score–transformed [46].

Statistical analysis

Data are shown as means ± SD or SEM of at least three independent samples. $P < 0.05$ was considered to be statistically significant. Significance is indicated as $^{*}P < 0.05$, $^{**}P < 0.01$, $^{***}P < 0.001$, or $^{****}P < 0.0001$; where necessary for clarity, lack of significance is indicated (ns). P values for comparisons between every pairwise combination among sample groups were obtained using the unpaired t-test with Welch's correction using GraphPad Prism version 7.0 for Windows (GraphPad Software Inc., San Diego, CA, U.S.A.).

Results

Licochalcone A is a PRMT6 inhibitor

In a previous report, we described the identification of licochalcone A as a broad-spectrum PRMT inhibitor at a concentration of 200 μM [38]. The structure of licochalcone A, a chalcone derivative, is shown in Figure 1A. To further understand the specificity of licochalcone A on histone arginine methyltransferases, we performed

Biochemical Journal (2021) **478** 389–406
https://doi.org/10.1042/BCJ20200411

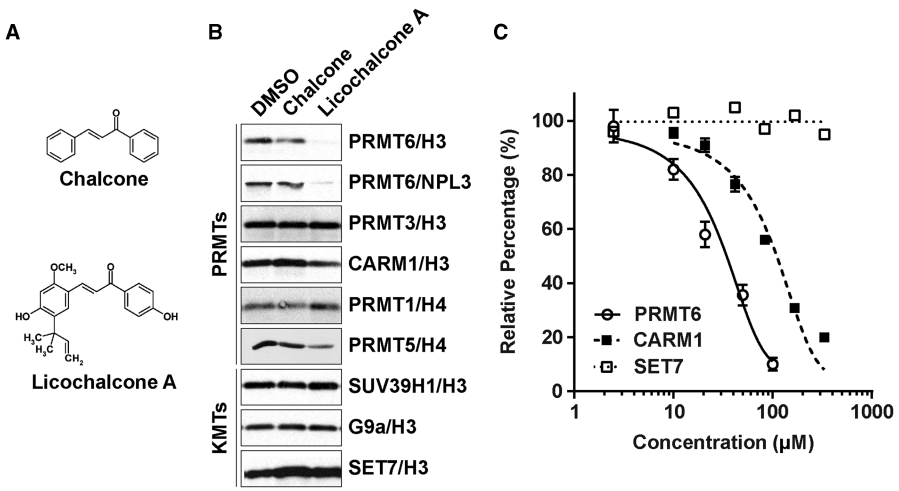

Figure 1. Inhibitory effects of licochalcone A on a set of methyltransferases.

(**A**) Chemical structure of chalcone and its analog, licochalcone A. (**B**) Inhibitory activity of chalcone and licochalcone A against PRMT6 using histone H3 and NPL3 as substrates and against a panel of arginine (PRMT1, PRMT3, CARM1, and PRMT5) and lysine (SUV39H1, SET7, and G9a) methyltransferases using their histone substrates. Substrates (0.5–1 μg) were incubated with recombinant enzymes (0.3 μg) in the presence of [^{3}H]AdoMet and 50 μM of chalcone or licochalcone A for 90 min at 30°C in 1× PBS (final volume 30 μl). A control reaction was performed in the presence of DMSO at 3.3% (v/v). Reactions were resolved by SDS–PAGE, transferred to a PVDF membrane, sprayed with Enhance (NEN) and exposed to film, overnight. (**C**) Determination IC_{50} values of licochalcone A. An *in vitro* methylation assay was established to determine the IC_{50} of licochalcone A. Dose-dependent curves showing licochalcone A inhibits PRMT6 and CARM1 activity but not SET7. Curve fitting and determination of IC_{50} by GraphPad, the calculated IC_{50} values are 22.3 μM for PRMT6 (solid curve), 68.8 μM for CARM1 (dashed curve), and more than 333.3 μM for SET7 (dotted curve). The data are presented as the mean ± S.E.M. $n = 3$.

an *in vitro* methylation assay using purified PRMT1, PRMT3, PRMT5, PRMT6, and CARM1 that have been reported to methylate histones [38] in the presence of a lower concentration of licochalcone A (50 μM) (Figure 1B). DMSO treated samples were included as controls (Figure 1B). A non-histone substrate of PRMT6 was also used to determine if licochalcone A acts by inhibiting PRMT6 enzyme rather than by targeting a specific substrate. We observed that in comparison with DMSO or chalcone treatment, licochalcone A treatment caused an almost complete loss of methylation of histone H3 and NPL3 proteins (Figure 1B). In contrast, the ability of PRMT1 and PRMT3 to methylate histone H4 and H3 remained unaffected, respectively, whereas a small reduction in the methylation of histone H3 by CARM1 was noted in samples exposed to licochalcone A (Figure 1B). PRMT5-dependent methylation of histone H4 also exhibited a slight decline in response to licochalcone A (Figure 1B). *In vitro* methylation assays were also performed to confirm the specificity of licochalcone A towards PRMTs. To this end, a similar reaction was performed with histone lysine methyl transferases (HKMTs) — SUV39H1, G9a and Set7 — with histone H3 as a substrate. As shown in Figure 1B, licochalcone A did not have a discernable effect on the methylation of histone H3 by these enzymes.

Next, we also performed *in vitro* methylation assays to compare the licochalcone A concentration (IC_{50}) at which a 50% reduction in the activities of CARM1, PRMT6, and SET7 against histone H3. As shown in Figure 1C, the IC_{50} values against CARM1 and PRMT6 (Type I PRMTs) were roughly 69 and 22 μM, respectively. We failed to achieve an IC_{50} dose of licochalcone A dose against the SET7 even when tested at concentrations up to 333 μM (Figure. 1C). These results indicate that licochalcone A is a more selective inhibitor of PRMT6 activity compared with other histone arginine methyltransferases.

Licochalcone A is a reversible and competitive PRMT6 inhibitor

We next performed a preincubation/dilution assay to study the mode of inhibition of PRMT6 by licochalcone A [47]. To this end, we preincubated 200 μM human GST-PRMT6 with 2 mM licochalcone A for 1 h, which is ∼70-fold its IC_{50} concentration. The expectation was that with more than 99% of the enzyme in an enzyme-inhibitor complex at this drug dose, and PRMT6 activity would have been inhibited. DMSO or 2 μM

Biochemical Journal (2021) **478** 389–406
https://doi.org/10.1042/BCJ20200411

of each compound was mixed with 200 nM PRMT6 directly to react with histone H3 for 1 h as the controls. Interestingly, a 1000-fold dilution of the preincubated mixture of PRMT6 and licochalcone A into 1xPBS reaction buffer with substrate histone H3 for 1 h reaction, resulted in restoration of ∼100% of PRMT6 activity compared with controls (Figure 2A). A similar experiment conducted with CARM1 and histone H3, also promoted a nearly 95% recovery of enzymatic activity, indicating licochalcone A is a reversible inhibitor of CARM1 against histone H3 as well (Supplementary Figure S1). Next, a Lineweaver-Burk plot was generated to study the kinetics of PRMT6 inhibition by licochalcone A. The increasing slope of lines with increasing licochalcone A concentrations and their intersection on the y-axis, suggest that licochalcone A is a competitive inhibitor of PRMT6 (Figure 2B). UV cross-linking assays were then performed to evaluate if licochalcone A interfered with AdoMet binding or substrate binding [44]. Cross-linking result was monitored by fluorography and ponceau staining of radiolabeled GST-PRMT6 (Figure 2C). We observed that licochalcone A did not prevent radiolabeled AdoMet binding, in contrast with the broad-spectrum methyl transferase inhibitors, sinefungin and AMI-5, which have been reported [44] to bind to the AdoMet binding site and therefore, served as positive controls. These results clearly demonstrate that licochalcone A inhibition does not involve the AdoMet binding site and strongly indicate that its mode of action likely involves insertion into the arginine-binding pocket of PRMT6 to compete with substrates. Together, these findings suggest that licochalcone A is a reversible, and a competitive PRMT6 inhibitor.

Licochalcone A inhibits PRMT6 activity in cells

To further confirm that PRMT6 is a direct binding target of licochalcone A in intact cells, we performed cellular thermal shift assay (CETSA) using MCF-7 cells [45]. As shown in Figure 3A, PRMT6 protein levels from licochalcone A treated cells were more stable to increase in temperature when compared with the control group, indicating potent binding of licochalcone A with PRMT6 to induce its thermal stabilization. A significant difference in CARM1 levels between treated and control groups was not noted in the same assay, suggesting licochalcone A is more specific to PRMT6 (Figure 3A). Pretreatment of MCF-7 cells with licochalcone A showed an obvious 3.9°C right shifts in the melting curves of PRMT6, but not CARM1 (Figure 3B,C). Thus, PRMT6 is confirmed as the direct binding target of licochalcone A in living cells.

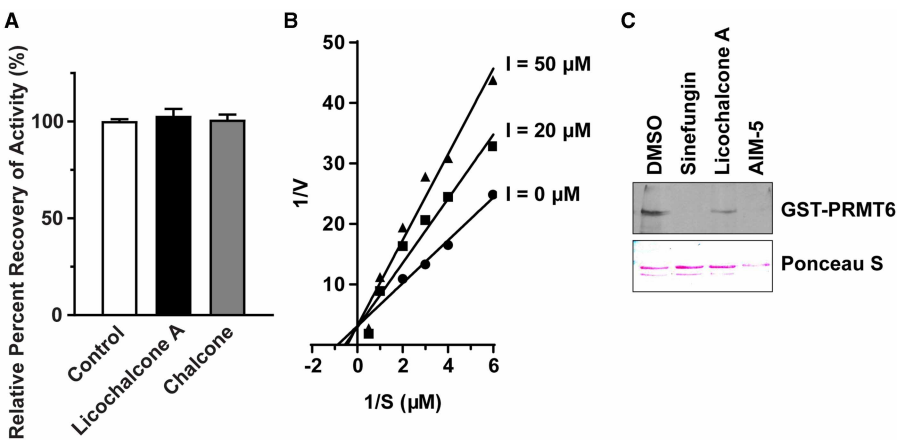

Figure 2. Licochalcone A is a reversible and competitive inhibitor.

(**A**) Licochalcone A is a reversible inhibitor. A dilution experiment was performed, where 200 μM GST-PRMT6 enzyme with 2 mM chalcone or licochalcone A were preincubated for 60 min, respectively, and then diluted 1000-fold into reaction mix at final 200 nM GST-PRMT6 and 2 μM of compound with substrate histone H3 for 1 h reaction. DMSO and 2 μM of each compound was mixed with 200 nM PRMT6 directly to react for 1 h as the controls. The relative percent recovery of PRMT6 activity compared with the control was calculated from three independent experiments. The data are presented as the mean ± S.E.M. (**B**) Typical Linweaver-Burke plots for inhibition of PRMT6 by licochalcone A. (**C**) Licochalcone A does not compete for AdoMet binding to PRMT6. An AdoMet UV cross-linking experiment was performed in the presence of potential competitors: 200 μM sinefungin, 200 μM licochalcone A, and 200 μM AMI-5. Samples were separated on a 10% SDS–PAGE, transferred to a PVDF membrane, sprayed with Enhance (NEN), and exposed to film overnight. Fluorographic results are shown and Ponceau S staining of the same membrane serves as a loading control.

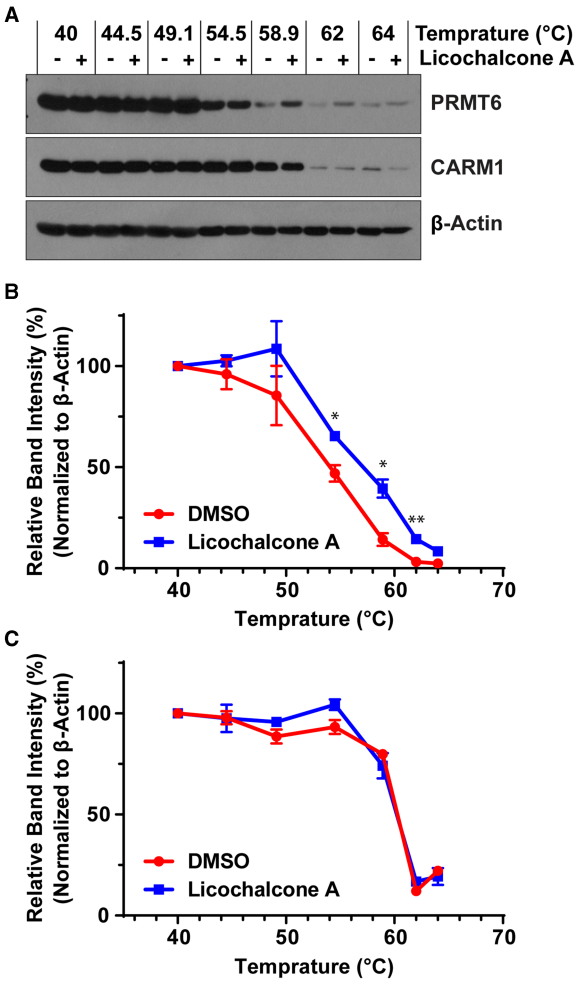

Figure 3. Licochalcone A binding to PRMT6 in cells.

Cellular thermal shift assay (CETSA) was used to evaluate the binding capability of licochalcone A with CARM1 and PRMT6. (**A**) MCF-7 cells were incubated with 40 μM licochalcone A for 24 h and then CETSA was performed. Representative PRMT6 and CARM1 Western blots of each sample are shown to demonstrate that licochalcone A increases the thermal stability of PRMT6, but not CARM1 in intact cells. (**B** and **C**) PRMT6 and CARM1 levels were normalized to β-actin levels that were used as a loading control. CETSA curves in intact cells for PRMT6 and CARM1 with licochalcone A are generated from triplicate independent experiments. The data are presented as the mean ± SD ($n = 3$) * $P < 0.05$ and ** $P < 0.01$ compared with control groups).

To determine whether licochalcone A inhibits histone H3 arginine 2 methylation (H3R2me2a) by PRMT6 in cells, two separate experiments were performed taking into consideration various technical caveats. First, the rate of turnover for histone methyl marks is much slower than that of histone acetylation [48]. The existence of arginine demethylases is controversial [2]. For these reasons, arginine methylation is a relatively stable methyl-mark and turnover of methylated substrates may take longer. Thus, a potential for lack of meaningful information with short drug treatment times along with possible inaccessibility of histones to the drug led us to develop a new method to increase the sensitivity to detect significant changes in protein methylation. Here, MCF-7 cells were first treated with cycloheximide and Chloramphenicol for 18 h to inhibit new protein synthesis and to bring about a reduction in the levels of pre-existing methylated proteins. Culture media was then changed to allow new protein synthesis, including histone H3. Licochalcone A was then added to the cells for 48 h of treatment and methylation of newly synthesized histones was monitored by Western blotting of acid-extracted histones, using methyl-specific antibodies. As seen in Figure 4A, licochalcone A caused a significant

Biochemical Journal (2021) **478** 389–406
https://doi.org/10.1042/BCJ20200411

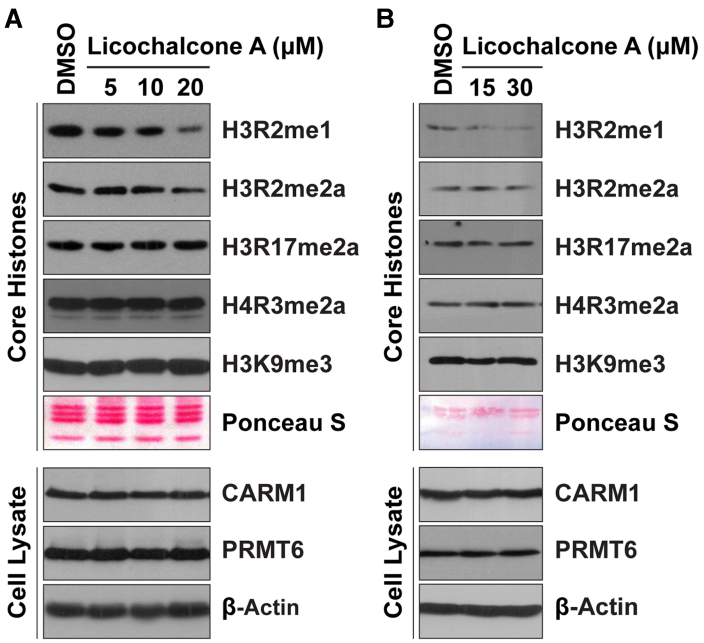

Figure 4. Licochalcone A inhibits histone H3R2 methylation in cells.

(**A**) MCF-7 cells were treated with cycloheximide (100 μg/ml in ethanol) and chloramphenicol (40 μg/ml) for 18 h to inhibit protein synthesis, and then new medium with indicated concentration of licochalcone A was added to the cells for additional 48 h treatment. Acid-extracted core histones from both control and treated cells were run and separated on 15% SDS–PAGE gels, transferred to a PVDF membranes, and then immunoblotted with indicated methyl-specific antibodies. Equal loading of core histones was monitored with Ponceau S staining (upper panel). Expression levels of PRMT6 and CARM1 in the whole-cell lysate were monitored using PRMT6 and CARM1 antibodies respectively with β-actin serving as a loading control (lower panel). (**B**) MCF-7 cells were treated with indicated doses of licochalcone A for 5 days. Acid-extracted core histones were purified and separated on 15% SDS–PAGE gels, transferred to a PVDF membrane, and then immunoblotted with indicated methyl-specific antibodies. Ponceau S staining indicates equal loading of core histones (upper panel). Expression levels of PRMT6 and CARM1 in the whole cell lysate were monitored using PRMT6 and CARM1 antibodies respectively with β-actin serving as a loading control (lower panel).

and dose-dependent decrease in H3R2 monomethylation. However, asymmetric dimethylation of H3R2 was reduced to a smaller extent (Figure 4A). An inhibitory effect of licochalcone A on histone H4R3 methylation was not observed in Western blots probed with H4R4me2a methyl-specific antibody (Figure 4A). Since PRMT6 and PRMT1 are both reported to methylate H4R3 *in vitro* [8,49], we assessed the effect of PRMT1 knockout on methylation of H4R3 in PRMT1-inducible cells. H4R3 methylation was almost completely abrogated under these conditions, indicating that PRMT1 is the primary enzyme that methylates this site (Supplementary Figure S2). This result also indicated that licochalcone A has no inhibitory activity against PRMT1 on the methylation of H4R3 at the tested concentration (Supplementary Figure S2). Licochalcone A has been shown to inhibit CARM1 activity in a cell-based reporter system [38]. However, the methylation of histone H3R17 site, a major site methylated by CARM1, was not affected by licochalcone A treatment (Figure 4A). Licochalcone A treatment did not alter the tri-methylation of histone H3K9, which is catalyzed by lysine methyl transferases, Suv39H1 and SETDB1 (Figure 4A). Finally, licochalcone A treatment did not affect levels of either PRMT6 or CARM1 (Figure 4A).

The inhibitory effects of licochalcone A on H3R2 methylation were further assessed by directly treating MCF-7 cells for 5 days. H3R2 monomethylation level was significantly inhibited in a dose-dependent manner by licochalcone A (Figure 4B). However, longer time treatment did not result in any significant decreases in the asymmetric dimethylation levels of H3R2 (Figure 4B). Licochalcone A-dependent reduction in levels of PRMT6 or CARM1, as well as that of H4R3me2a, H3R17me2a, and H3K9me3, were not noted, suggesting that licochalcone A is a selective inhibitor of H3R2 methylation in cells (Figure 4B).

Biochemical Journal (2021) 478 389–406
https://doi.org/10.1042/BCJ20200411

Licochalcone A inhibits estrogen receptor-mediated gene activation and selectively decreases the viability of MCF-7 cells

Recently, PRMT6 was identified as a transcriptional coactivator of the nuclear receptor, estrogen receptor-alpha (ER-α) in breast cancer cells [17]. We, therefore, mined the transcriptome information publicly available at the Gene Expression Omnibus GEO database with submission number GSE29431 to assess PRMT6 expression levels in human breast cancer samples. First, we found *PRMT6* gene expression to be significantly up-regulated in primary carcinoma samples relative to normal breast tissues (Figure 5A). Second, its up-regulated expression was significantly associated with tumor malignancy and an advanced tumor staging status (Figure 5B). These findings suggest that PRMT6 may be a driver of breast cancer development and a potential therapeutic target. To test this possibility, we examined the effect of licochalcone A treatment on the coactivity of PRMT6 in MCF-7 cells. To this end, cells were transfected with Myc-tagged PRMT6 and estrogen response element (ERE) luciferase reporter, followed by treatment with different concentrations of licochalcone A for 36 h. The dual luciferase assay performed to evaluate the inhibitory effect of compound on reporter gene expression induction by estradiol revealed a licochalcone A dose-dependent decline in reporter activity from ERE (Figure 5C). Next, to rule out the possibility that the inhibitory effects of licochalcone A on ERE reporter was due to CARM1 inactivation, we knocked down CARM1 expression using tetracycline-inducible *CARM1* shRNA and the dual luciferase assay was repeated as described above. CARM1 was significantly knocked down as shown by Western blotting analysis (Figure 5D). Surprisingly, the expression of transiently transfected PRMT6 was elevated 2-fold or more in MCF-7 cells with *CARM1* knockdown, which was associated with a 2-fold increase in ERE reporter activity in licochalcone A-treated cells relative to untreated controls (Figure 5D). These data suggest that the increase in reporter activity was not only CARM1-dependent, but also PRMT6-dependent. Licochalcone A can inhibit the coactivator activity of PRMT6 in a dose-dependent manner similarly to what we observed in parental MCF-7 cells without CARM1 knockdown, suggesting licochalcone A might directly target PRMT6 to exhibit its activity (Figure 5C). To further characterize the effect of licochalcone A on endogenous genes, we focused on the well-characterized ERα target genes, GREB1 and TFF1 [43,50,51]. MCF-7 cells were estrogen starved in phenol red-free DMEM for 4 days and treated with E2 and licochalcone A. Using quantitative RT-PCR (qRT-PCR), we confirmed that GREB1 and TFF1 expression was significantly activated upon addition of E2 to MCF-7 cells, but not control GAPDH expression (Figure 5E). Licochalcone A significantly inhibited the E2-induced expression of GREB1 and TFF1 genes in a dose-dependent manner (Figure 5E). GAPDH gene expression was not significant changed following treatment even at 40 μM of licochalcone A (Figure 5E). These results demonstrate that the ER transcriptional activity facilitated by PRMT6 can be suppressed by licochalcone A. To further investigate the selectivity of licochalcone A on cytotoxicity towards breast cancer cells, we compared the effect of a 5-day drug exposure on the viability of MCF-7 breast cancer cells and MCF-10A non-tumorigenic breast epithelial cells using the CellTiter-Glo Luminescent Cell Viability Assay. A significant and dose-dependent reduction was observed upon licochalcone A treatment (Figure 5F). In contrast, growth reduction in MCF-10A cells was not noted even at a dose of 30 μM licochalcone A, indicating that the drug has preferential cytotoxicity against breast cancer cells (Figure 5F).

Licochalcone A induces G2/M arrest in breast cancer cells

To determine the basis for the specific toxicity of licochalcone A against MCF-7 breast cancer cells, we performed flow cytometry to assess the cell cycle distribution of MCF-7 and MCF-10A cells after treatment with 10 μM, 30 μM, and 40 μM licochalcone A for 48 h. We observed a dose-dependent G2/M accumulation of both MCF-7 and MCF-10 A cells following licochalcone A treatment (Figure 6A–C). An increase in the percentage of MCF-7 cells at G2/M was seen with increasing licochalcone A concentrations, as was coupled with a decrease in the proportion of cells in G1 and S phases (Figures 6A upper panel & 6B). In contrast, the percentage of MCF-10A cells at G2/M phase was associated with a decrease in the number of cells in G1 and a slightly increase in the proportion of cells in S phase of the cell cycle (Figure 6A-bottom panel & 6C). In the absence of drug treatment, ∼7.23% and 10.3% of MCF-7 and MCF-10A cells, respectively, were found in G2/M. Treatment with 30 μM and 40 μM licochalcone A caused a substantial increase in the number of MCF-7 (24.9% and 28.7%) and MCF-10A (15.0% and 18.8%) cells in G2/M. Thus, MCF-7 cells had a 2.4 and 2.2-fold increase, respectively, in cells with a G2/M DNA content compared with MCF-10A cells. These data demonstrate that licochalcone A is more effective in inducing G2/M arrest against MCF-7 cell than normal breast MCF-10A cell.

Biochemical Journal (2021) **478** 389–406
https://doi.org/10.1042/BCJ20200411

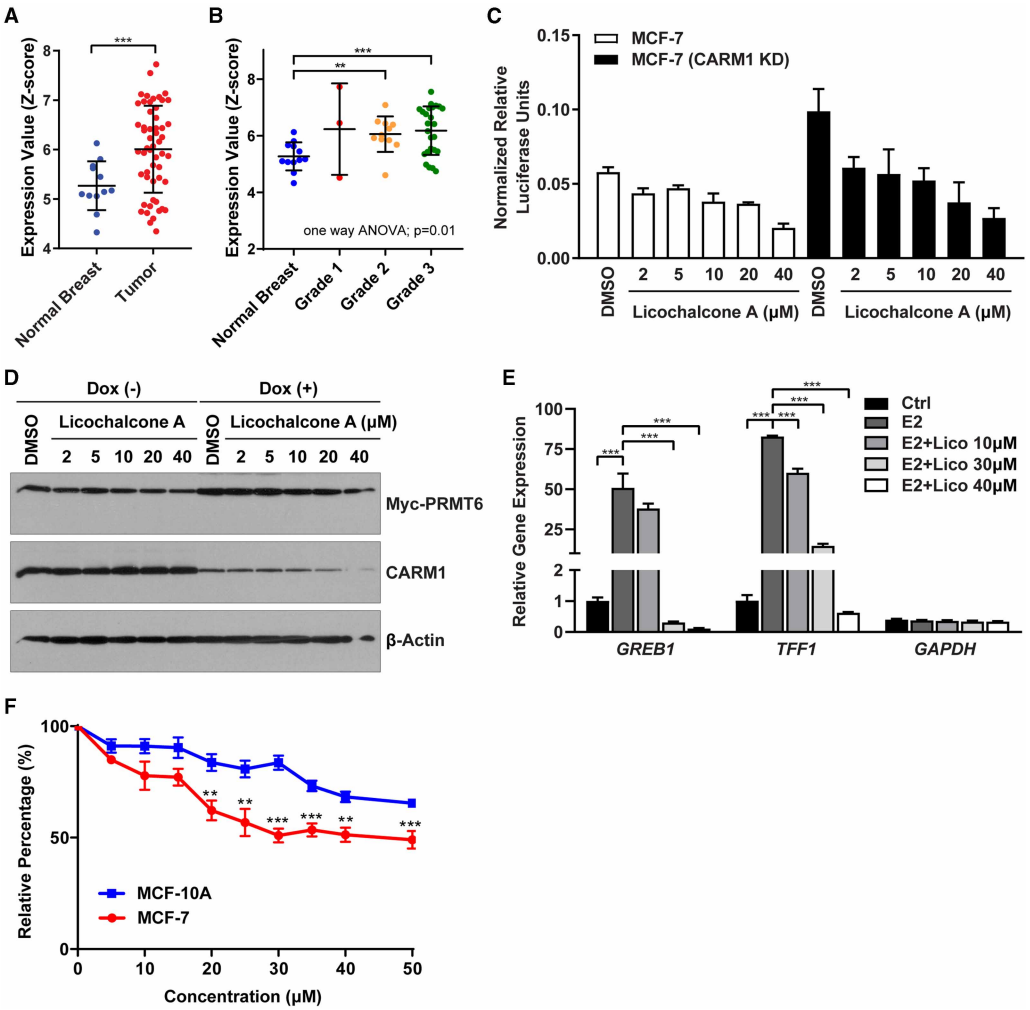

Figure 5. Inhibitory effects of licochalcone A on estrogen receptor-mediated transcriptional activation in MCF-7 cells.

Part 1 of 2

(**A**) PRMT6 gene expression profiles measured by expression microarray in 15 normal breast samples and 54 breast carcinoma samples. Each dot corresponds to one individual. Data show individual variability and means ± SD. * $P < 0.05$, ** $P < 0.01$, *** $P < 0.001$, **** $P < 0.0001$. (**B**) PRMT6 gene expression profiles measured in normal breast samples and breast carcinoma samples (Grade 1, $n = 3$; Grade 2, $n = 11$; Grade 3, $n = 25$). (**C**) ERE-Luc reporter activity is repressed in MCF-7 cells with licochalcone A treatment. MCF-7 and Dox-inducible CARM1 knockdown MCF-7 cells were cultured in phenol red-free DMEM supplemented with 10% charcoal dextran-stripped FBS for 3 days, and then transiently transfected with 250 ng of ERE-LUC, 200 ng of pSG-GRIP1, 200 ng of pVAX-PRMT6, and 2 ng humanized CMV-Renilla internal control. After 12 h of transfection, cells were treated with 20 nM E2 to induce ERE-firefly and the indicated amount of licochalcone A for 36 h. Relative activity of firefly luciferase was normalized against Renilla luciferase activity, and the results are represented as mean ± SD calculated from triplicate luciferase experiments. (**D**) Cell lysates taken from Luciferase assays were separated on 10% SDS–PAGE gels, transferred to a PVDF membrane, and then immunoblotted with Myc and CARM1 antibodies to monitor the expression levels of Myc-PRMT6 and endogenous CARM1 in different groups of treatment. β-actin serves as a loading control. (**E**) MCF-7 cells were cultured in phenol red-free DMEM supplemented with 10% charcoal dextran-stripped FBS for 4 days and treated with the indicated amount of licochalcone A. After 24 h of incubation, media were replaced and the cells were treated with E2 (20 nM) and licochalcone A for another 24 h. Total RNA was extracted and RT-PCR was performed using primers specific for the genes shown. GAPDH acts as a negative control. Target gene expression was normalized to β-actin. Error bars represent standard deviation based on three independent experiments. * $P < 0.05$, ** $P < 0.01$ and *** $P < 0.001$. (**F**) MCF-7 and MCF-10A cells were exposed to various concentrations of the licochalcone A (0, 5, 10, 15, 20, 25, 30, 35, 40, and 50 μM) respectively for 4 days followed by analysis using the CellTiter-Glo Luminescent Cell Viability Assay to

Figure 5. Inhibitory effects of licochalcone A on estrogen receptor-mediated transcriptional activation in MCF-7 cells. Part 2 of 2

measure ATP as an indication of cell viability. The results are represented mean ± S.E.M. of four independent experiments. $^{**}P < 0.01$ and $^{***}P < 0.001$ vs DMSO control.

Comparative analysis of apoptosis induced by licochalcone A in MCF-7 and MCF-10A cells

Although licochalcone A is known to induce apoptosis in MCF-7 cells, a comparative study with non-tumorigenic MCF-10A breast epithelial cells not been conducted [35–37]. To this end, annexin V/7-AAD double staining assay was conducted and the number of apoptotic cells was quantified using a flow cytometric analysis. Cells stained with Annexin V+/7-AAD+ were defined as late apoptotic or dead cells, while cells stained with annexin V+/7-AAD− were considered to be in early stages of apoptosis. As shown in Figure 7A,B, at 48 h of exposure, the number of early apoptotic cells MCF-7 cells (Annexin V+/7-AAD−) increased from 5.35% (DMSO control) to 6.69%,16.2%, and 27.5% with licochalcone A concentrations of 10 μM, 30 μM, and 40 μM, respectively. A significant difference in early apoptosis was not observed between untreated and treated

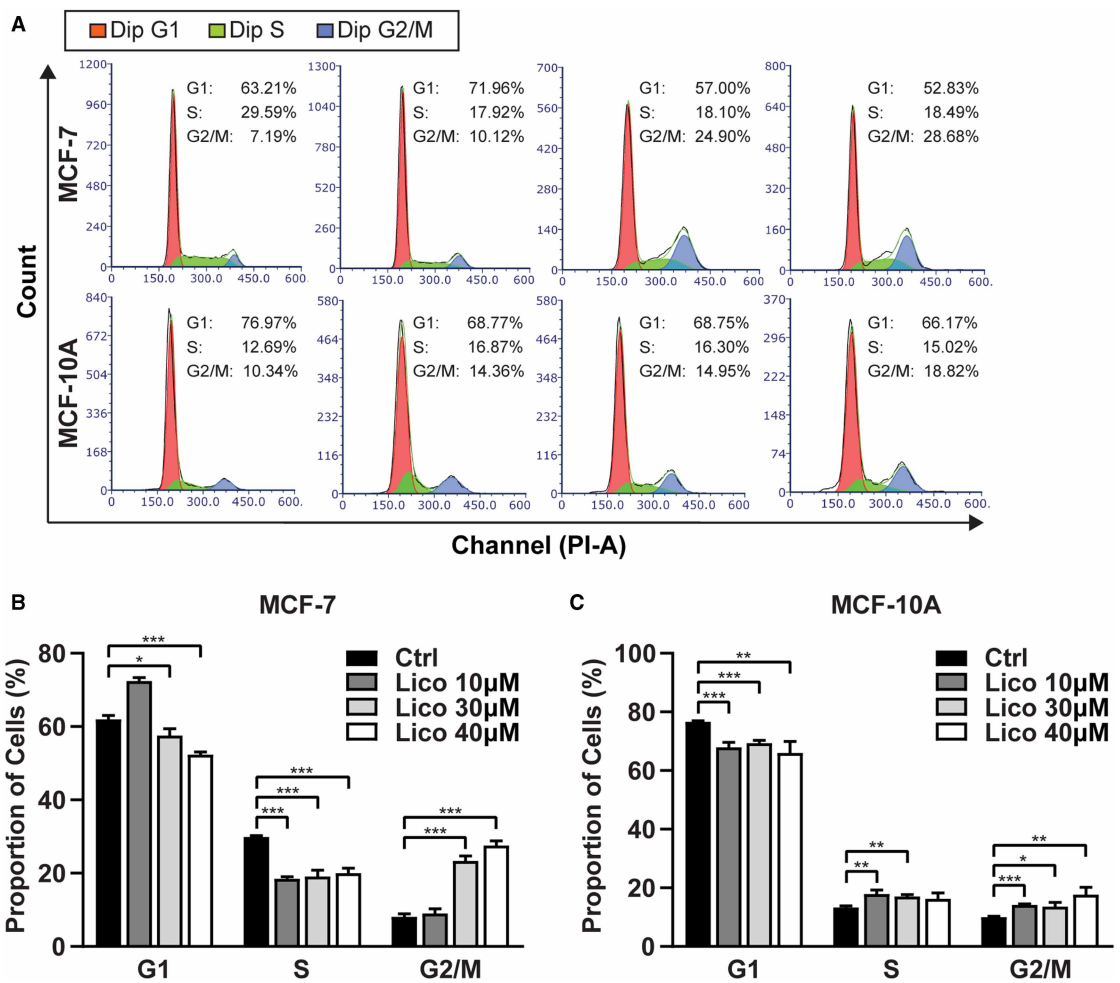

Figure 6. Effects of licochalcone A on cell cycle analysis.

(**A**) MCF-7 and MCF-10A Cells were treated with indicated licochalcone A for 48 h and the cell cycle distribution was analyzed by flow cytometry. (**B** and **C**) Percentages of cells in each cell-cycle phase. The data are presented as mean ± SD of three independent experiments ($n = 3$). * $P < 0.05$, ** $P < 0.01$, and *** $P < 0.001$ compared with untreated cells.

Biochemical Journal (2021) **478** 389–406
https://doi.org/10.1042/BCJ20200411

in MCF-10 A cells. Overall, a 1.3-, 3.0-, and 5.1-fold increase in early apoptotic cells was seen in MCF-7 cells compared with the MCF-10A cells. Compared with 1.23% of late apoptotic/dead MCF-7 cells (Annexin V +/7-AAD+) in DMSO treated samples, treatment with 10 μM, 30 μM, and 40 μM licochalcone A for 48 h promoted a 1.3-, 4.8-, and 8.1-fold increase (1.58%, 5.86%, and 18.1%), in the number of late apoptotic/dead cells. In contrast, only 0.31% MCF-10A cells were in the late stages of apoptosis in vehicle treated samples, as outlined for MCF7 cells, caused a small, but significant increase in the percentage of late apoptotic/dead cells (1.19% and 1.58%, respectively) in 30 μM and 40 μM licochalcone A treated samples. This translates roughly to a 3.8- and 5-fold increase in late apoptotic/dead cells relative to the vehicle treated samples.

Overall, licochalcone A (40 μM) caused a substantially larger increase in apoptosis or death in MCF7 cells (45.6%) compared with MCF-10A cells (3.4%). Taken together, our results indicate that licochalcone A promotes a G2/M phase arrest in both cells, but continues on to induce apoptosis in MCF-7 cells, highlighting its enhanced cytotoxicity towards breast cancer cells (Figure 7A,B).

Licochalcone A abrogates PRMT6-dependent reduction in p53 in MCF-7 cells

We next investigated the mechanism by which licochalone A induced apoptosis in MCF-7 cells. As stated earlier, p53 is a target of the repressive activity of PRMT6. Therefore, we asked if inhibition of PRMT6 activity can increase p53 levels and induce apoptosis in MCF-7 cells. First, Western blot analyses were performed to determine the levels of p53 and PRMT6 proteins in MCF-7 and MCF-10A cells following treatment with 10 μM, 30 μM, and 40 μM licochalcone A for 48 h. As shown in Figure 7C and consistent with a previous report [52], p53 protein levels are substantially lower in MCF-7 cancer cells compared with MCF-10A human mammary epithelial cells. Licochalcone A treatment increased p53 levels in MCF-7 cells in a concentration-dependent manner, but not in MCF-10A cells (Figure 7C).

Consistent with p53 being a target of PRMT6, levels of the latter were higher in MCF-7 cells relative to MCF-10A cells (Figure 7C). Licochalcone A did not affect the expression levels of PRMT6 in MCF-7 and MCF-10A cells (Figure 7C). Cleavage of PARP is a hallmark of apoptosis [53,54]. Exposure to 10 μM, 30 μM, and 40 μM licochalcone A for 48 h resulted in a dose-dependent increase in cleavage of PARP in MCF-7A cells (Figure 7C). In MCF-10A cells, PARP cleavage was not detected with 10 μM and 30 μM licochalcone A treatment, but weak cleavage could be seen at 40 μM drug (Figure 7C). These findings show that MCF-7 is more sensitive to induce apoptotic death by licochalcone A than that of MCF-10A cells.

To establish the involvement of PRMT6 in licochalcone A-induced cell apoptosis or death, in MCF-7 cells, we asked if apoptosis could be rescued by ectopic PRMT6 expression. MCF-7 cells treated with licochalcone A were transiently transfected with pCAGGS-PRMT6 vector expressing FLAG-tagged PRMT6 and flow cytometry performed to compare the levels of annexin V/7-AAD double staining. The number of early and late apoptotic/dead cells were defined as described previously. Treatment with 35 μM licochalcone A increased early apoptosis from 3.16% to 22.0% in untransfected cells and from 2.26% in control vector to only 7.25%, a 3-fold decrease in apoptosis, in FLAG-PRMT6 expressing cells (Figure 7D,E). PRMT6 expression also caused a 2.3-fold reduction in licochalcone A induced late apoptosis and death in MCF-7 cells (0.12% to 1.14%) compared with 0.1% to 2.67% in control untransfected cells (Figure 7D,E).

Western blot assays were also performed to demonstrate a reduced up-regulation of p53 protein levels in response to PRMT6 overexpression (Figure 7F). Taken together, these results indicate that licochalcone A induces apoptosis in MCF-7 cell partially by inhibiting PRMT6 activity.

Discussion

Expression of the arginine methyl transferase PRMT6 is elevated in breast cancer and is correlated with poor prognostic significance for patients [26–28]. Indeed, our study confirmed these observations using a different human breast cancer patient dataset. Furthermore, we also found PRMT6 levels to be associated with higher tumor grade (Figure 5B). An oncogenic role for PRMT6 in breast cancer development was demonstrated by Bao et al. using a genetically engineered mouse model [29]. These data are further supported by work from another group, which has shown that growth of breast cancers *in vivo* could be blocked by PRMT6 depletion [27,29]

PRMT6 can methylate histone H3 as well as non-histone substrates. It transcriptionally represses p53 through histone H3R2 methylation [11]. PRMT6 inhibits the growth suppressive functions of p16 and p21 not only by transcriptional repression, but also by methylation to change p16 protein conformation and to increase cytoplasmic localization of p21 [22,55]. PRMT6 overexpression promotes the activity of the oncogenic PI3K/AKT pathway, possibly by methylating ERα at arginine 260 [29]. Both PRMT1 and PRMT6 methylate ERα at

Biochemical Journal (2021) **478** 389–406
https://doi.org/10.1042/BCJ20200411

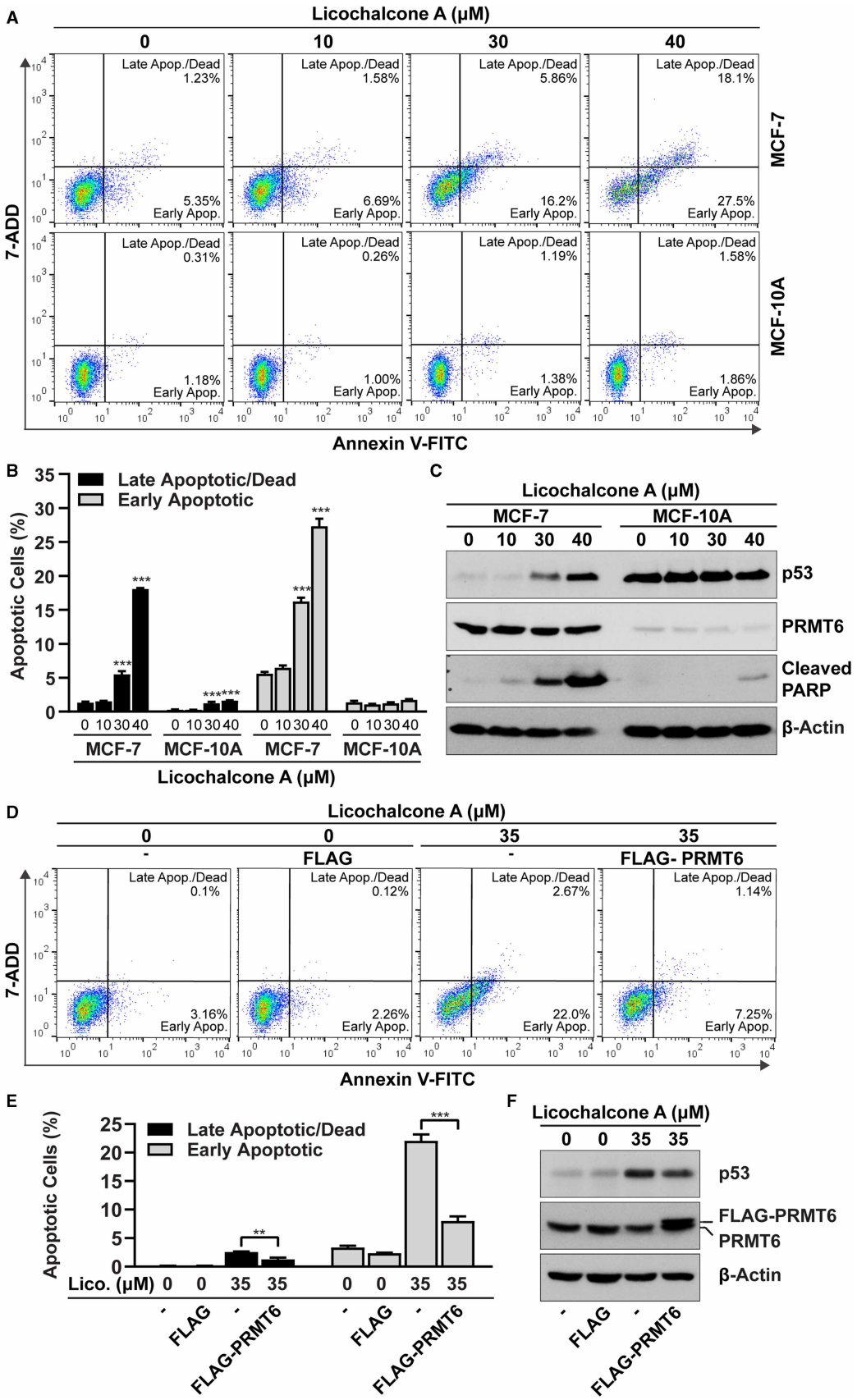

Figure 7. Induction of apoptosis by licochalcone A in MCF-7 and MCF-10A cells. Part 1 of 2

(**A**) To identify licochalcone A-induced apoptosis, flow cytometry analysis was performed by Annexin V and 7-AAD staining.

Biochemical Journal (2021) **478** 389–406
https://doi.org/10.1042/BCJ20200411

Figure 7. Induction of apoptosis by licochalcone A in MCF-7 and MCF-10A cells. Part 2 of 2

The percentage of annexin V+/7-AAD+ (late apoptotic/dead) cells, in the top right quadrant, and annexin V+/PI– (early apoptotic) cells, in the bottom right quadrant, are indicated. (**B**) Bar graphs illustrating the percentage of late apoptotic/dead and early apoptotic cells in MCF-7 and MCF-10A cells treated with indicated amount of licochalcone A for 48 h. The data are presented as mean ± SD of three independent experiments ($n = 3$). *** $P < 0.001$ compared with untreated cells. (**C**) MCF-7 and MCF-10A cells were treated with the indicated concentrations of licochalcone A for 48 h. Whole-cell extracts were immunoblotted with the indicated antibodies. β-actin serves as a loading control. (**D**) A rescue experiment was performed whereby wild-type FLAG-PRMT6 construct was reintroduced into licochalcone A treated MCF-7 cells. MCF-7 cells were treated with DMSO and 35 μM licochalcone A alone or in combination with transfection of a control plasmid or plasmid containing FLAG-PRMT6 for 24 h. Flow cytometry analysis of annexin V/7-AAD double staining was carried out to examine the number of apoptotic cells. The percentage of annexin V+/7-AAD+ (late apoptotic/dead) cells, in the top right quadrant, and annexin V+/PI– (early apoptotic) cells, in the bottom right quadrant, are indicated. (**E**) Bar graphs illustrating the percentage of late apoptotic/dead and early apoptotic cells at the indicated treatments. The data are presented as mean ± SD of three independent experiments ($n = 3$). ** $P < 0.01$ and *** $P < 0.001$. (**F**) Cell lysates taken from rescue experiment (**D**) were immunoblotted with p53 and PRMT6 antibodies to examined for p53 expression and the expression levels of FLAG-PRMT6 and endogenous PRMT6 in different groups of treatment. β-actin serves as a loading control.

this site [4,56]. In addition to the coactivator of estrogen receptor, PRMT6 also coactivates the progesterone, glucocorticoid and androgen receptors in a methylation-dependent manner [17,57]. PRMT6 regulates alternative splicing [17,28] and PTEN methylation is thought to be regulated by PRMT6 through such a mechanism [23], Thus, PRMT6 appears to play an important role in regulating multiple aspects of gene expression including transcription and alternative splicing, cellular functions that are known to be perturbed during carcinogenesis [28].

These lines of evidence indicating an oncogenic function for PRMT6 led us to investigate if PRMT6-specific inhibitors could be developed for anti-cancer therapy. Our previous work has identified licochalcone A as a PRMT inhibitor [38]. Licochalcone A is one of the main active components in licorice, a commonly used herbal medicine in Asia. It is a product of the dried root and rhizomes of Glycyrrhiza uralensis Fisch., G. glabra L., and G. inflata Bat. [58]. It is frequently prescribed in traditional Chinese medicine (TCM) for enhancing the efficacy of other TCMs and/or decreasing their toxicity [59,60]. Recent studies have reported multiple pharmacological attributes to licorice, including anti-viral, anti-microbial, anti-inflammation, anti-cancer properties [34,35,61–66]. *In vivo* studies with osteosarcoma, glioma, gastric cancer, colon and cervical cancers revealed reduction in tumor burden in mouse models following induction of apoptosis in response to licochalcone A treatment, although the target of its inhibitory activity has not clearly been demonstrated [61,64,66–68].

Here, we identified licochalcone A as the first naturally occurring, selective, and reversible inhibitor of PRMT6 (Figure 1). It is a competitive inhibitor, but does not compete for the SAM binding site of PRMT6 (Figure 2). Although, a previous study had shown inhibition of CARM1 by licochalcone A in an induced FLAG-PABP1 cellular reporter system, which was also noted in our studies, inhibition of CARM1 by licochalcone A required significantly higher drug doses. This observation was also confirmed by CETSA assays, which revealed PRMT6 to be a preferred target for licochalcone A (Figure 3). Additional support for this result was also derived from our finding that licochalcone A inhibits histone H3R2 methylation which can be catalyzed by PRMT6 (Figure 4), but not histone H3R17 methylation, which is mainly brought about by CARM1 [69].

Licochalcone A has been shown to induce apoptosis of breast cancer cells *in vitro* and block breast cancer growth in mouse model [34–37]. These pathways are also known to be affected by PRMT6. For example, licochalcone A decreased the viability of MCF-7 cells by inhibiting PI3K/Akt/mTOR activation, a pathway known to be activated by PRMT6 overexpression, and promoted induction of caspase-dependent apoptosis [29,35]. PRMT6 synergistically functions with Steroid Receptor Coactivator (SRC-1) to coactivate ERα [17,56], which is in line with our observation identifying PRMT6 involvement in the reduction in ERE reporter activity and the expression of endogenous estrogen-responsive genes in response to licochalcone A treatment (Figure 5C,E). Knockdown of PRMT6 levels by siRNA interference is known to cause an estrogen-dependent decrease in proliferation of MCF-7 cells [17], which is also supported by our findings that licochalcone A promotes a preferential reduction in proliferation of MCF-7 cells relative to normal MCF-10A breast epithelial cells (Figure 5F).

PRMT6 promotes histone arginine methylation at the p53 locus to silence p53 gene expression [11]. In line with this, our data showed that p53 protein level is lower in MCF-7 cells than that of MCF-10A cells, which is also consistent with a previous report [52], and this negatively corelated with the expression of PRMT6 (Figure 7C). An inverse correlation between PRMT6 and p53 levels in MCF-7 and MCF-10A cells provides further support for a link between these proteins in licochalcone A-induced cell death of MCF-7 cells. Other reports have suggested that a subset of chalcones up-regulate p53 protein levels in MCF-7 cells [70,71], although similar studies have not been conducted with licochalcone A. Indeed, drug-induced up-regulation of p53, drove apoptosis following a G2/M cycle arrest in MCF-7 cells as opposed to MCF-10A cells, where licochalcone A treatment caused a G2/M arrest, but failed to trigger apoptosis (Figure 7). These findings suggest that licochalcone A can target cancer cells and possibly spare normal cells. Licochalcone A also induced p53 expression in HCT116 human colon cancer cells and SGC-7901 human gastric cancer cells [72,73]. A growing body of evidence suggests that licochalcone A acts through multiple targets to induce apoptosis [35,36,73]. PRMT6 appears to be an important target of the drug because constitutive expression of PRMT6 could reverse licochalcone A-induced apoptosis in MCF7 cells. Thus, while our data suggest that licochalcone A targets PRMT6 activity, and acts by p53 up-regulation, current evidence also indicates that licochalcone A and PRMT6 can modulate signaling through multiple pathways. Thus, additional studies are needed to determine if p53-independent mechanisms are also deployed by PRMT6 to attenuate breast cancer cell growth. Therefore, a better understanding of the anti-tumor activity of licochalcone A in the specific context of PRMT6 function, is necessary.

Our *in vitro* studies suggest that licochalcone A has therapeutic potential against breast cancer. However, future *in vivo* studies are needed in patient derived xenograft models of triple negative breast cancers to investigate if their higher levels of PRMT6, which we have shown in this study, makes them uniquely sensitive to licochalcone A treatment. There is also a need for further efforts to identify potent and selective PRMT6 inhibitors. As a first step in this direction, we have synthesized new compounds that are based on licochalcone A and previously designed pharmacophore structures [74] for identifying potent and selective PRMT6 inhibitors (Supplementary Figure S3). Recently reported Aryl Pyrazoles and MS117 are promising PRMT6 inhibitors [30,31]. However, its transition from a tool compound to a therapeutic modality requires further mechanistic analyses.

Finally, in addition to PRMT6, expression of a number of other PRMTs is up-regulated in cancers, making them appealing targets for therapeutics development [2]. Indeed, one PRMT1 and three PRMT5 inhibitors have entered into Phase I clinical trials for solid and hematological tumors between 2016 to 2019 [75]. We anticipate that PRMT inhibitors will constitute the next wave of epigenetic modifiers to make the transition from the laboratory space to clinical testing.

Competing Interests

The authors declare that there are no competing interests associated with the manuscript.

Funding

This work was supported by the Addis Faith Foundation (V.G.) and NIH P20GM109005 (G.Z.).

CRediT Contribution

Donghang Cheng: Conceptualization, Resources, Data curation, Formal analysis, Supervision, Validation, Investigation, Visualization, Writing — original draft, Project administration, Writing — review and editing. **Shuai Gong:** Resources, Data curation, Formal analysis, Validation, Investigation, Visualization, Methodology, Writing — review and editing. **Shinji Maegawa:** Data curation, Software, Formal analysis, Investigation, Visualization, Methodology. **Yanwen Yang:** Resources, Validation, Investigation, Visualization, Methodology. **Vidya Gopalakrishnan:** Conceptualization, Resources, Data curation, Supervision, Funding acquisition, Writing — original draft, Project administration, Writing — review and editing. **Guangrong Zheng:** Conceptualization, Resources, Data curation, Supervision, Funding acquisition, Investigation, Writing — original draft, Writing — review and editing.

Biochemical Journal (2021) **478** 389–406
https://doi.org/10.1042/BCJ20200411

Acknowledgements

We thank Dr. Vidya Vemulapalli and Ms. Cari Sagum for critical reading of manuscript and language editing.

Abbreviations

ADMA, asymmetric dimethylarginine; CETSA, cellular thermal shift assay; DMEM, Dulbecco's Modified Eagle's Medium; DMSO, dimethyl sulfoxide; ERE, estrogen response element; PI, propidium iodide; PRMT, protein arginine methyltransferases; SAM, S-adenosyl L-methionine; TSP-1, Thrombospondin-1.

References

1 Bedford, M.T. and Clarke, S.G. (2009) Protein arginine methylation in mammals: who, what, and why. *Mol. Cell* **33**, 1–13 https://doi.org/10.1016/j.molcel.2008.12.013
2 Yang, Y. and Bedford, M.T. (2013) Protein arginine methyltransferases and cancer. *Nat. Rev. Cancer* **13**, 37–50 https://doi.org/10.1038/nrc3409
3 Frankel, A., Yadav, N., Lee, J., Branscombe, T.L., Clarke, S. and Bedford, M.T. (2002) The novel human protein arginine N-methyltransferase PRMT6 is a nuclear enzyme displaying unique substrate specificity. *J. Biol. Chem.* **277**, 3537–3543 https://doi.org/10.1074/jbc.M108786200
4 Avasarala, S., Wu, P.Y., Khan, S.Q., Yanlin, S., Van Scoyk, M., Bao, J. et al. (2020) PRMT6 promotes lung tumor progression via the alternate activation of tumor-associated macrophages. *Mol. Cancer Res.* **18**, 166–178 https://doi.org/10.1158/1541-7786.MCR-19-0204
5 Singhroy, D.N., Mesplede, T., Sabbah, A., Quashie, P.K., Falgueyret, J.P. and Wainberg, M.A. (2013) Automethylation of protein arginine methyltransferase 6 (PRMT6) regulates its stability and its anti-HIV-1 activity. *Retrovirology* **10**, 73 https://doi.org/10.1186/1742-4690-10-73
6 Lakowski, T.M. and Frankel, A. (2008) A kinetic study of human protein arginine N-methyltransferase 6 reveals a distributive mechanism. *J. Biol. Chem.* **283**, 10015–10025 https://doi.org/10.1074/jbc.M710176200
7 Guccione, E., Bassi, C., Casadio, F., Martinato, F., Cesaroni, M., Schuchlautz, H. et al. (2007) Methylation of histone H3R2 by PRMT6 and H3K4 by an MLL complex are mutually exclusive. *Nature* **449**, 933–937 https://doi.org/10.1038/nature06166
8 Hyllus, D., Stein, C., Schnabel, K., Schiltz, E., Imhof, A., Dou, Y. et al. (2007) PRMT6-mediated methylation of R2 in histone H3 antagonizes H3 K4 trimethylation. *Genes Dev.* **21**, 3369–3380 https://doi.org/10.1101/gad.447007
9 Iberg, A.N., Espejo, A., Cheng, D., Kim, D., Michaud-Levesque, J., Richard, S. et al. (2008) Arginine methylation of the histone H3 tail impedes effector binding. *J. Biol. Chem.* **283**, 3006–3010 https://doi.org/10.1074/jbc.C700192200
10 Gong, W., Suzuki, K., Russell, M. and Riabowol, K. (2005) Function of the ING family of PHD proteins in cancer. *Int. J. Biochem. Cell Biol.* **37**, 1054–1065 https://doi.org/10.1016/j.biocel.2004.09.008
11 Neault, M., Mallette, F.A., Vogel, G., Michaud-Levesque, J. and Richard, S. (2012) Ablation of PRMT6 reveals a role as a negative transcriptional regulator of the p53 tumor suppressor. *Nucleic Acids Res.* **40**, 9513–9521 https://doi.org/10.1093/nar/gks764
12 Chu, M.C., Selam, F.B. and Taylor, H.S. (2004) HOXA10 regulates p53 expression and matrigel invasion in human breast cancer cells. *Cancer Biol. Ther.* **3**, 568–572 https://doi.org/10.4161/cbt.3.6.848
13 Lim, Y., Yu, S., Yun, J.A., Do, I.G., Cho, L., Kim, Y.H. et al. (2018) The prognostic significance of protein arginine methyltransferase 6 expression in colon cancer. *Oncotarget* **9**, 9010–9020 https://doi.org/10.18632/oncotarget.23809
14 Michaud-Levesque, J. and Richard, S. (2009) Thrombospondin-1 is a transcriptional repression target of PRMT6. *J. Biol. Chem.* **284**, 21338–21346 https://doi.org/10.1074/jbc.M109.005322
15 Kazerounian, S., Yee, K.O. and Lawler, J. (2008) Thrombospondins in cancer. *Cell. Mol. Life Sci.* **65**, 700–712 https://doi.org/10.1007/s00018-007-7486-z
16 Cheng, D., Gao, G., Di Lorenzo, A., Jayne, S., Hottiger, M.O., Richard, S. et al. (2020) Genetic evidence for partial redundancy between the arginine methyltransferases CARM1 and PRMT6. *J. Biol. Chem.* **295**, 17060–17070 https://doi.org/10.1074/jbc.RA120.014704
17 Harrison, M.J., Tang, Y.H. and Dowhan, D.H. (2010) Protein arginine methyltransferase 6 regulates multiple aspects of gene expression. *Nucleic Acids Res.* **38**, 2201–2216 https://doi.org/10.1093/nar/gkp1203
18 Miranda, T.B., Webb, K.J., Edberg, D.D., Reeves, R. and Clarke, S. (2005) Protein arginine methyltransferase 6 specifically methylates the nonhistone chromatin protein HMGA1a. *Biochem. Biophys. Res. Commun.* **336**, 831–835 https://doi.org/10.1016/j.bbrc.2005.08.179
19 Sgarra, R., Lee, J., Tessari, M.A., Altamura, S., Spolaore, B., Giancotti, V. et al. (2006) The AT-hook of the chromatin architectural transcription factor high mobility group A1a is arginine-methylated by protein arginine methyltransferase 6. *J. Biol. Chem.* **281**, 3764–3772 https://doi.org/10.1074/jbc.M510231200
20 El-Andaloussi, N., Valovka, T., Toueille, M., Hassa, P.O., Gehrig, P., Covic, M. et al. (2007) Methylation of DNA polymerase beta by protein arginine methyltransferase 1 regulates its binding to proliferating cell nuclear antigen. *FASEB J.* **21**, 26–34 https://doi.org/10.1096/fj.06-6194com
21 Stein, C., Riedl, S., Ruthnick, D., Notzold, R.R. and Bauer, U.M. (2012) The arginine methyltransferase PRMT6 regulates cell proliferation and senescence through transcriptional repression of tumor suppressor genes. *Nucleic Acids Res.* **40**, 9522–9533 https://doi.org/10.1093/nar/gks767
22 Nakakido, M., Deng, Z., Suzuki, T., Dohmae, N., Nakamura, Y. and Hamamoto, R. (2015) PRMT6 increases cytoplasmic localization of p21CDKN1A in cancer cells through arginine methylation and makes more resistant to cytotoxic agents. *Oncotarget* **6**, 30957–30967 https://doi.org/10.18632/oncotarget.5143
23 Feng, J., Dang, Y., Zhang, W., Zhao, X., Zhang, C., Hou, Z. et al. (2019) PTEN arginine methylation by PRMT6 suppresses PI3K-AKT signaling and modulates pre-mRNA splicing. *Proc. Natl Acad. Sci. U.S.A.* **116**, 6868–6877 https://doi.org/10.1073/pnas.1811028116
24 El-Andaloussi, N., Valovka, T., Toueille, M., Steinacher, R., Focke, F., Gehrig, P. et al. (2006) Arginine methylation regulates DNA polymerase beta. *Mol. Cell* **22**, 51–62 https://doi.org/10.1016/j.molcel.2006.02.013
25 Veland, N., Hardikar, S., Zhong, Y., Gayatri, S., Dan, J., Strahl, B.D. et al. (2017) The arginine methyltransferase PRMT6 regulates DNA methylation and contributes to global DNA hypomethylation in cancer. *Cell Rep.* **21**, 3390–3397 https://doi.org/10.1016/j.celrep.2017.11.082

26 Yoshimatsu, M., Toyokawa, G., Hayami, S., Unoki, M., Tsunoda, T., Field, H.I. et al. (2011) Dysregulation of PRMT1 and PRMT6, type I arginine methyltransferases, is involved in various types of human cancers. *Int. J. Cancer* **128**, 562–573 https://doi.org/10.1002/ijc.25366
27 Phalke, S., Mzoughi, S., Bezzi, M., Jennifer, N., Mok, W.C., Low, D.H. et al. (2012) p53-Independent regulation of p21Waf1/Cip1 expression and senescence by PRMT6. *Nucleic Acids Res.* **40**, 9534–9542 https://doi.org/10.1093/nar/gks858
28 Dowhan, D.H., Harrison, M.J., Eriksson, N.A., Bailey, P., Pearen, M.A., Fuller, P.J. et al. (2012) Protein arginine methyltransferase 6-dependent gene expression and splicing: association with breast cancer outcomes. *Endocr. Relat. Cancer* **19**, 509–526 https://doi.org/10.1530/ERC-12-0100
29 Bao, J., Di Lorenzo, A., Lin, K., Lu, Y., Zhong, Y., Sebastian, M.M. et al. (2019) Mouse models of overexpression reveal distinct oncogenic roles for different type I protein arginine methyltransferases. *Cancer Res.* **79**, 21–32 https://doi.org/10.1158/0008-5472.CAN-18-1995
30 Mitchell, L.H., Drew, A.E., Ribich, S.A., Rioux, N., Swinger, K.K., Jacques, S.L. et al. (2015) Aryl pyrazoles as potent inhibitors of arginine methyltransferases: identification of the first PRMT6 tool compound. *ACS Med. Chem. Lett.* **6**, 655–659 https://doi.org/10.1021/acsmedchemlett.5b00071
31 Shen, Y., Li, F., Szewczyk, M.M., Halabelian, L., Park, K.S., Chau, I. et al. (2020) Discovery of a first-in-class protein arginine methyltransferase 6 (PRMT6) covalent inhibitor. *J. Med. Chem.* **63**, 5477–5487 https://doi.org/10.1021/acs.jmedchem.0c00406
32 Eram, M.S., Shen, Y., Szewczyk, M., Wu, H., Senisterra, G., Li, F. et al. (2016) A potent, selective, and cell-active inhibitor of human type I protein arginine methyltransferases. *ACS Chem. Biol.* **11**, 772–781 https://doi.org/10.1021/acschembio.5b00839
33 Wang, Z.F., Liu, J., Yang, Y.A. and Zhu, H.L. (2020) A review: the anti-inflammatory, anticancer and antibacterial properties of four kinds of licorice flavonoids isolated from licorice. *Curr. Med. Chem.* **27**, 1997–2011 https://doi.org/10.2174/0929867325666181001104550
34 Huang, W.C., Su, H.H., Fang, L.W., Wu, S.J. and Liou, C.J. (2019) Licochalcone A inhibits cellular motility by suppressing E-cadherin and MAPK signaling in breast cancer. *Cells* **8**, 218 https://doi.org/10.3390/cells8030218
35 Xue, L., Zhang, W.J., Fan, Q.X. and Wang, L.X. (2018) Licochalcone A inhibits PI3K/Akt/mTOR signaling pathway activation and promotes autophagy in breast cancer cells. *Oncol. Lett.* **15**, 1869–1873 https://doi.org/10.3892/ol.2017.7451
36 Kang, T.H., Seo, J.H., Oh, H., Yoon, G., Chae, J.I. and Shim, J.H. (2017) Licochalcone A suppresses specificity protein 1 as a novel target in human breast cancer cells. *J. Cell Biochem.* **118**, 4652–4663 https://doi.org/10.1002/jcb.26131
37 Bortolotto, L.F., Barbosa, F.R., Silva, G., Bitencourt, T.A., Beleboni, R.O., Baek, S.J. et al. (2017) Cytotoxicity of trans-chalcone and licochalcone A against breast cancer cells is due to apoptosis induction and cell cycle arrest. *Biomed. Pharmacother.* **85**, 425–433 https://doi.org/10.1016/j.biopha.2016.11.047
38 Cheng, D. and Bedford, M.T. (2011) Xenoestrogens regulate the activity of arginine methyltransferases. *Chembiochem* **12**, 323–329 https://doi.org/10.1002/cbic.201000522
39 Weiss, V.H., McBride, A.E., Soriano, M.A., Filman, D.J., Silver, P.A. and Hogle, J.M. (2000) The structure and oligomerization of the yeast arginine methyltransferase, Hmt1. *Nat. Struct. Biol.* **7**, 1165–1171 https://doi.org/10.1038/78941
40 O'Carroll, D., Scherthan, H., Peters, A.H., Opravil, S., Haynes, A.R., Laible, G. et al. (2000) Isolation and characterization of Suv39h2, a second histone H3 methyltransferase gene that displays testis-specific expression. *Mol. Cell. Biol.* **20**, 9423–9433 https://doi.org/10.1128/MCB.20.24.9423-9433.2000
41 Wang, H., Cao, R., Xia, L., Erdjument-Bromage, H., Borchers, C., Tempst, P. et al. (2001) Purification and functional characterization of a histone H3-lysine 4-specific methyltransferase. *Mol. Cell* **8**, 1207–1217 https://doi.org/10.1016/S1097-2765(01)00405-1
42 Tachibana, M., Sugimoto, K., Fukushima, T. and Shinkai, Y. (2001) Set domain-containing protein, G9a, is a novel lysine-preferring mammalian histone methyltransferase with hyperactivity and specific selectivity to lysines 9 and 27 of histone H3. *J. Biol. Chem.* **276**, 25309–25317 https://doi.org/10.1074/jbc.M101914200
43 Cheng, D., Vemulapalli, V., Lu, Y., Shen, J., Aoyagi, S., Fry, C.J. et al. (2018) CARM1 methylates MED12 to regulate its RNA-binding ability. *Life Sci. Alliance* **1**, e201800117 https://doi.org/10.26508/lsa.201800117
44 Cheng, D., Yadav, N., King, R.W., Swanson, M.S., Weinstein, E.J. and Bedford, M.T. (2004) Small molecule regulators of protein arginine methyltransferases. *J. Biol. Chem.* **279**, 23892–23899 https://doi.org/10.1074/jbc.M401853200
45 Martinez Molina, D., Jafari, R., Ignatushchenko, M., Seki, T., Larsson, E.A., Dan, C. et al. (2013) Monitoring drug target engagement in cells and tissues using the cellular thermal shift assay. *Science* **341**, 84–87 https://doi.org/10.1126/science.1233606
46 Lopez, F.J., Cuadros, M., Cano, C., Concha, A. and Blanco, A. (2012) Biomedical application of fuzzy association rules for identifying breast cancer biomarkers. *Med. Biol. Eng. Comput.* **50**, 981–990 https://doi.org/10.1007/s11517-012-0914-8
47 Copeland, R.A. (2005) Evaluation of enzyme inhibitors in drug discovery. A guide for medicinal chemists and pharmacologists. *Methods Biochem. Anal.* **46**, 1–265 PMID:16350889
48 Ng, S.S., Yue, W.W., Oppermann, U. and Klose, R.J. (2009) Dynamic protein methylation in chromatin biology. *Cell. Mol. Life Sci.* **66**, 407–422 https://doi.org/10.1007/s00018-008-8303-z
49 Wang, H., Huang, Z.Q., Xia, L., Feng, Q., Erdjument-Bromage, H., Strahl, B.D. et al. (2001) Methylation of histone H4 at arginine 3 facilitating transcriptional activation by nuclear hormone receptor. *Science* **293**, 853–857 https://doi.org/10.1126/science.1060781
50 Kocanova, S., Kerr, E.A., Rafique, S., Boyle, S., Katz, E., Caze-Subra, S. et al. (2010) Activation of estrogen-responsive genes does not require their nuclear co-localization. *PLoS Genet.* **6**, e1000922 https://doi.org/10.1371/journal.pgen.1000922
51 Metivier, R., Penot, G., Hubner, M.R., Reid, G., Brand, H., Kos, M. et al. (2003) Estrogen receptor-alpha directs ordered, cyclical, and combinatorial recruitment of cofactors on a natural target promoter. *Cell* **115**, 751–763 https://doi.org/10.1016/S0092-8674(03)00934-6
52 Li, Q., Hao, Q., Cao, W., Li, J., Wu, K., Elshimali, Y. et al. (2019) PP2Cdelta inhibits p300-mediated p53 acetylation via ATM/BRCA1 pathway to impede DNA damage response in breast cancer. *Sci. Adv.* **5**, eaaw8417 https://doi.org/10.1126/sciadv.aaw8417
53 Kaufmann, S.H., Desnoyers, S., Ottaviano, Y., Davidson, N.E. and Poirier, G.G. (1993) Specific proteolytic cleavage of poly(ADP-ribose) polymerase: an early marker of chemotherapy-induced apoptosis. *Cancer Res.* **53**, 3976–3985 PMID:8358726
54 Tewari, M., Quan, L.T., O'Rourke, K., Desnoyers, S., Zeng, Z., Beidler, D.R. et al. (1995) Yama/CPP32 beta, a mammalian homolog of CED-3, is a crmA-inhibitable protease that cleaves the death substrate poly(ADP-ribose) polymerase. *Cell* **81**, 801–809 https://doi.org/10.1016/0092-8674(95)90541-3
55 Wang, X., Huang, Y., Zhao, J., Zhang, Y., Lu, J. and Huang, B. (2012) Suppression of PRMT6-mediated arginine methylation of p16 protein potentiates its ability to arrest A549 cell proliferation. *Int. J. Biochem. Cell Biol.* **44**, 2333–2341 https://doi.org/10.1016/j.biocel.2012.09.015

Biochemical Journal (2021) **478** 389–406
https://doi.org/10.1042/BCJ20200411

56 Sun, Y., Chung, H.H., Woo, A.R. and Lin, V.C. (2014) Protein arginine methyltransferase 6 enhances ligand-dependent and -independent activity of estrogen receptor alpha via distinct mechanisms. *Biochim. Biophys. Acta* **1843**, 2067–2078 https://doi.org/10.1016/j.bbamcr.2014.04.008
57 Scaramuzzino, C., Casci, I., Parodi, S., Lievens, P.M.J., Polanco, M.J., Milioto, C. et al. (2015) Protein arginine methyltransferase 6 enhances polyglutamine-expanded androgen receptor function and toxicity in spinal and bulbar muscular atrophy. *Neuron* **85**, 88–100 https://doi.org/10.1016/j.neuron.2014.12.031
58 Wang, L., Yang, R., Yuan, B., Liu, Y. and Liu, C. (2015) The antiviral and antimicrobial activities of licorice, a widely-used Chinese herb. *Acta Pharm. Sin. B* **5**, 310–315 https://doi.org/10.1016/j.apsb.2015.05.005
59 Guo, J., Shang, E., Zhao, J., Fan, X., Duan, J., Qian, D. et al. (2014) Data mining and frequency analysis for licorice as a 'Two-Face' herb in Chinese formulae based on Chinese formulae database. *Phytomedicine* **21**, 1281–1286 https://doi.org/10.1016/j.phymed.2014.07.006
60 Wang, X., Zhang, H., Chen, L., Shan, L., Fan, G. and Gao, X. (2013) Liquorice, a unique 'guide drug' of traditional Chinese medicine: a review of its role in drug interactions. *J. Ethnopharmacol.* **150**, 781–790 https://doi.org/10.1016/j.jep.2013.09.055
61 Hao, W., Yuan, X., Yu, L., Gao, C., Sun, X., Wang, D. et al. (2015) Licochalcone A-induced human gastric cancer BGC-823 cells apoptosis by regulating ROS-mediated MAPKs and PI3K/AKT signaling pathways. *Sci. Rep.* **5**, 10336 https://doi.org/10.1038/srep10336
62 Choi, A.Y., Choi, J.H., Hwang, K.Y., Jeong, Y.J., Choe, W., Yoon, K.S. et al. (2014) Licochalcone A induces apoptosis through endoplasmic reticulum stress via a phospholipase Cgamma1-, Ca^{2+}-, and reactive oxygen species-dependent pathway in HepG2 human hepatocellular carcinoma cells. *Apoptosis* **19**, 682–697 https://doi.org/10.1007/s10495-013-0955-y
63 Lee, C.S., Kwak, S.W., Kim, Y.J., Lee, S.A., Park, E.S., Myung, S.C. et al. (2012) Guanylate cyclase activator YC-1 potentiates apoptotic effect of licochalcone A on human epithelial ovarian carcinoma cells via activation of death receptor and mitochondrial pathways. *Eur. J. Pharmacol.* **683**, 54–62 https://doi.org/10.1016/j.ejphar.2012.03.024
64 Lu, W.J., Wu, G.J., Chen, R.J., Chang, C.C., Lien, L.M., Chiu, C.C. et al. (2018) Licochalcone A attenuates glioma cell growth in vitro and in vivo through cell cycle arrest. *Food Funct.* **9**, 4500–4507 https://doi.org/10.1039/C8FO00728D
65 Qiu, C., Zhang, T., Zhang, W., Zhou, L., Yu, B., Wang, W. et al. (2017) Licochalcone A inhibits the proliferation of human lung cancer cell lines A549 and H460 by inducing G2/M cell cycle arrest and ER stress. *Int. J. Mol. Sci.* **18**, 1761 https://doi.org/10.3390/ijms18081761
66 Shen, T.S., Hsu, Y.K., Huang, Y.F., Chen, H.Y., Hsieh, C.P. and Chen, C.L. (2019) Licochalcone A suppresses the proliferation of osteosarcoma cells through autophagy and ATM-Chk2 activation. *Molecules* **24**, 2435 https://doi.org/10.3390/molecules24132435
67 Kim, J.K., Shin, E.K., Park, J.H., Kim, Y.H. and Park, J.H. (2010) Antitumor and antimetastatic effects of licochalcone A in mouse models. *J. Mol. Med. (Berl)* **88**, 829–838 https://doi.org/10.1007/s00109-010-0625-2
68 Tsai, J.P., Lee, C.H., Ying, T.H., Lin, C.L., Lin, C.C., Hsueh, J.T. et al. (2015) Licochalcone A induces autophagy through PI3K/Akt/mTOR inactivation and autophagy suppression enhances Licochalcone A-induced apoptosis of human cervical cancer cells. *Oncotarget* **6**, 28851–28866 https://doi.org/10.18632/oncotarget.4767
69 Di Lorenzo, A. and Bedford, M.T. (2011) Histone arginine methylation. *FEBS Lett.* **585**, 2024–2031 https://doi.org/10.1016/j.febslet.2010.11.010
70 Santos, D., Bertholin Anselmo, M.B., de Oliveira, D., Jardim-Perassi, J.G., Alves Monteiro, B.V., Silva, D. et al. (2019) Antiproliferative activity and p53 upregulation effects of chalcones on human breast cancer cells. *J. Enzyme Inhib. Med. Chem.* **34**, 1093–1099 https://doi.org/10.1080/14756366.2019.1615485
71 Yu, L., Ma, J., Han, J., Wang, B., Chen, X., Gao, C. et al. (2016) Licochalcone B arrests cell cycle progression and induces apoptosis in human breast cancer MCF-7 cells. *Recent Pat. Anticancer Drug Discov.* **11**, 444–452 https://doi.org/10.2174/1574892811666160906091405
72 Lin, X., Tian, L., Wang, L., Li, W., Xu, Q. and Xiao, X. (2017) Antitumor effects and the underlying mechanism of licochalcone A combined with 5-fluorouracil in gastric cancer cells. *Oncol. Lett.* **13**, 1695–1701 https://doi.org/10.3892/ol.2017.5614
73 Yao, K., Chen, H., Lee, M.H., Li, H., Ma, W., Peng, C. et al. (2014) Licochalcone A, a natural inhibitor of c-Jun N-terminal kinase 1. *Cancer Prev. Res. (Phila)* **7**, 139–149 https://doi.org/10.1158/1940-6207.CAPR-13-0117
74 Mai, A., Valente, S., Cheng, D., Perrone, A., Ragno, R., Simeoni, S. et al. (2007) Synthesis and biological validation of novel synthetic histone/protein methyltransferase inhibitors. *ChemMedChem* **2**, 987–991 https://doi.org/10.1002/cmdc.200700023
75 Jarrold, J. and Davies, C.C. (2019) PRMTs and arginine methylation: cancer's best-Kept secret? *Trends Mol. Med.* **25**, 993–1009 https://doi.org/10.1016/j.molmed.2019.05.007